ARTICLES

Effects of Mn additions on the P embrittlement of the Fe grain boundary

Lieping Zhong
Department of Physics and Astronomy, Northwestern University, Evanston, Illinois 60208

Ruqian Wu
Department of Physics and Astronomy, California State University, Northridge, California 91330

A. J. Freeman
Department of Physics and Astronomy, Northwestern University, Evanston, Illinois 60208

G. B. Olson
Department of Materials Science and Engineering, Northwestern University, Evanston, Illinois 60208
(Received 26 November 1996)

To achieve an electronic level understanding of intergranular embrittlement and its control in steel, the first principles full potential linearized augmented plane wave method and the atomic force approach are used to investigate the effect of Mn additions and P impurities on the energetics and underlying electronic properties of both the Fe grain boundary (GB) and the corresponding intergranular fracture surface (FS). The calculated binding-energy difference is +0.17 eV/adatom for P in the P/Fe binary system, in agreement with its observed embrittlement potency. The Mn is also found to contribute a direct embrittling effect of +0.20 eV/adatom, associated with stronger Mn-Fe chemical bonding in the FS environment. The computed binding-energy difference for P in the (P+Mn)/Fe ternary system is increased to +0.40 eV/adatom, consistent with experimental evidence that Mn facilitates P embrittlement in the grain boundary. The origin of the Mn enhanced P embrittlement is attributed to the strengthened in-plane P-Mn interaction, which makes the P impurity interact more isotropically with the surrounding Mn and Fe atoms in the GB and FS. [S0163-1829(97)06117-1]

I. INTRODUCTION

The mechanical properties of ultra-high-strength steels are often limited by the cohesion of crystal grain boundaries (GB) as influenced by the intergranular segregation of various metalloid impurities such as P and S. Even infinitesimal amounts of these trace impurities in the bulk material can lead to dramatic decreases in overall toughness owing to their preferential segregation, and thus pose significant technological problems.[1] Fortunately, the segregated impurities are often associated with the presence of transition metal alloying elements which can have different, or even contrasting influences on the impurity produced embrittlement. For example, for a given P impurity segregation, Mn and Cr additions are reported to facilitate the embrittlement, but Mo and W additions are found to increase the overall GB fracture strength.[2] Such results suggest that it may be possible to remedy, or even eliminate, the embrittlement problem by judicious selection of alloying elements.

To this end, understanding the underlying mechanism of metalloid impurity embrittlement potency and the role of alloying elements of the transition series is of great importance, and thus has been the subject of considerable research effort. A thermodynamic theory developed by Rice and Wang[3] describes the mechanism of impurity induced embrittlement through the competition between dislocation crack blunting and brittle separation governing the propagation resistance of an intergranular crack. The most striking result of the analysis is the prediction of a correlation between the embrittling potency of impurities and the differ-

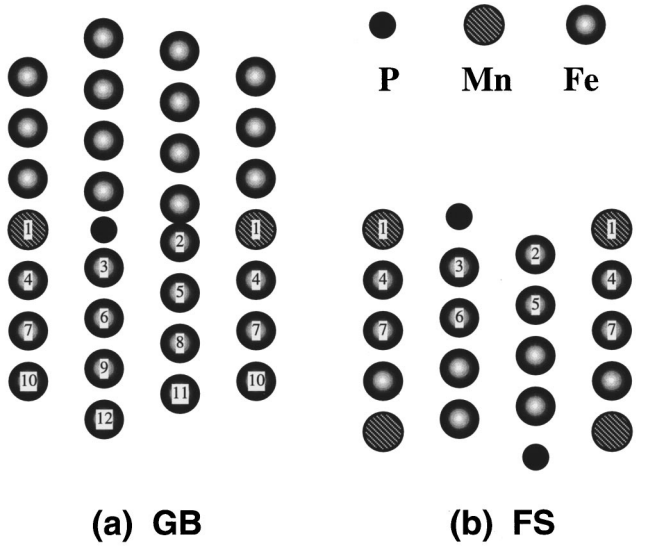

FIG. 1. Model and notation for the structures with Mn, P impurity at (left) the Fe $\Sigma 3[\bar{1}10]$ (111) grain boundary, and (right) the Fe(111) free surface.

TABLE I. Calculated interlayer distance in GB case starting from the grain boundary core (in a.u.).

Layer	Clean Fe GB	P/Fe GB	Mn/Fe GB(FM)	Mn/Fe GB(AFM)	(Mn+P)/Fe GB
d_{12}	2.10	2.21	2.05	2.26	2.17
d_{23}	1.27	1.69	1.30	1.02	1.76
d_{34}	1.50	1.19	1.52	1.57	1.12
d_{45}	1.61	1.54	1.62	1.64	1.57

ence between their segregation energies at free surfaces (FS) and at GB. Solutes with a lower energy at the FS reduce boundary cohesion, while those with a lower energy at the GB are cohesion enhancers.

Based on this hypothesis, electronic structure calculations are directed at determining the difference in energy and underlying electronic structure for segregating solutes at the GB and FS. Following early pioneering work[4–6] highly precise first principles methods, both by cluster[7] and band approaches,[8] have addressed this issue. By using the full-potential linearized augmented plane wave (FLAPW) approach, the underlying mechanism for the metalloid impurity (B,C,P,S) GB embrittlement has been attributed to (i) structural relaxation and (ii) the spatial anisotropy of the impurity-Fe bonds.[8]

To date, however, previous efforts have mainly focussed on binary systems composed of the metalloid impurity and Fe host elements. The role of ternary transition metal alloying on GB cohesion is much more complicated. Among the physics involved are the effects coming from the alloying element itself and the interaction between alloying elements and metalloid impurities. For both effects, electronic calculations can offer such useful information as the energetics and bonding character, and thus can be a powerful tool for revealing the underlying physical phenomena on the electronic level.

In order to provide an in-depth insight into the mechanisms of effects of impurities and their alloys on intergranular cohesion, we investigate the effects of the Mn ternary additions on the P embrittlement of the Fe GB by the highly precise FLAPW method within the total energy and atomic force approach. Following presentation of the model and computational details in Sec. II, the results of structural optimizations and magnetic interactions are discussed in Sec. III. The calculated segregation energy differences and finally the underlying chemical interactions, are discussed and conclusions given in Sec. IV.

II. MODEL AND COMPUTATION

As sketched in Fig. 1, a 23 layer slab is adopted to simulate the clean Fe$\Sigma 3[1\bar{1}0](111)$ GB;[9] the Mn additions replace Fe(1) in the GB core, the P impurity is placed in the trigonal prism formed by Fe and/or Mn atoms. With 12 atomic layers in-between, the influence of the surface (introduced artificially in the slab model) on the GB is expected to be sufficiently reduced so as to be negligible. For the FS, the corresponding Fe(111) substrate is simulated by a 13 layer slab. The P adsorbate is placed pseudomorphically on the threefold hollow sites on both sides of the slab, while Mn serves as a substitutional atom in the Fe(1) site. With sufficiently thick slab models, it is feasible to take structure relaxation into account for the GB and FS considered. The two-dimensional (2D) lattice constant and the unrelaxed Fe-Fe interatomic distance is chosen as the experimental value for bulk bcc Fe, i.e., $d_{\mathrm{Fe-Fe}}=4.69$ a.u. The structures within the (111) planes in both the GB and FS are kept unchanged for maintaining the in-plane symmetry; the three outermost Fe layer spacings in the GB are fixed in the bulk values to reduce free surface effects in the finite thickness slab. The final equilibrium geometry is determined by adjusting the vertical interplanar distances according to the calculated atomic forces[10] acting on the atoms.

As crucial reference systems, it is also very important to obtain highly precise results for the atomic structure and bonding properties of the binary Mn/Fe and P/Fe GB and FS. For the P/Fe systems, previous cluster calculations have shown that the surface effects are very strong even when the cluster consists of 93 atoms. Thus the equilibrium geometries of the GB systems determined by the DMol cluster method, as employed in our previous FLAPW calculation,[8] may not be applicable because of significant errors caused by surface effects in the finite cluster. Here, we reoptimize the structure of the P/Fe system within the FLAPW method and atomic force approach. Systematic error cancellations are expected because of the same treatment given to the ternary (P+Mn)/Fe and binary P/Fe and Mn/Fe reference systems.

In the FLAPW method,[11] no shape approximations are made to the charge densities, potentials, and matrix elements. The core states are treated fully relativistically and the valence states are treated semirelativistically (i.e., without spin-orbit coupling).[12] We employ the Hedin and Lundqvist and the von Barth and Hedin formulas for the exchange-

TABLE II. Calculated interlayer distance in FS case starting from the surface (in a.u.).

Layer	Clean Fe FS	P/Fe FS	Mn/Fe FS(FM)	Mn/Fe FS(AFM)	(Mn+P)/Fe
d_{P-1}		0.87			0.71
d_{12}	1.40	1.19	1.75	1.62	1.53
d_{23}	1.22	2.03	1.17	1.17	1.79
d_{34}	1.60	1.19	1.55	1.52	1.33
d_{45}	1.51	1.36	1.51	1.54	1.45

TABLE III. Calculated spin magnetic moments in the GB environment (in μ_B).

Atom	Fe GB	P/Fe GB	Mn/Fe GB	(Mn+P)/Fe GB
P		−0.03		−0.03
Fe(Mn)(1)	2.60	1.85	−3.00 [a]	2.15 [a]
Fe(2)	1.90	2.14	1.86	2.06
Fe(3)	2.28	1.78	2.18	1.81
Fe(4)	2.19	2.37	2.20	2.32
Fe(5)	2.18	2.21	2.19	2.17

[a]For Mn.

TABLE IV. Calculated spin magnetic moments in the FS environment (in μ_B).

Atom	Fe FS	P/Fe FS	Mn/Fe FS	(Mn+P)/Fe FS
P		−0.03		−0.04
Fe(Mn)(1)	2.73	1.77	−3.43 [a]	2.35 [a]
Fe(2)	2.20	2.20	2.01	2.06
Fe(3)	2.32	1.72	2.10	1.91
Fe(4)	2.15	2.20	2.02	2.22
Fe(5)	2.14	2.11	2.31	2.18

[a]For Mn.

correlation potentials for the nonmagnetic and the spin-polarized calculations, respectively.[13] Energy cutoffs of 13 and 100 Ry are employed for plane wave bases and star functions to describe the wave functions and the charge density and potential in the interstitial region, respectively. Within the muffin-tin (MT) spheres ($r_{\mathrm{MT,Fe}}=2.1$ a.u., $r_{\mathrm{MT,Mn}}=2.3$ a.u., $r_{\mathrm{MT,P}}=1.5$ a.u.), lattice harmonics with angular-momentum l up to 8 are adopted. Convergence is assumed when the average root-mean-square difference between the input and output charge and spin densities is less than 2×10^{-4} e/(a.u.)^3. In the self-consistent iterations, the step-forward approach[14] is used to speed up the calculation.

III. MAGNETISM AND ATOMIC STRUCTURE

We first examine the binary Mn/Fe system. Compared to the clean Fe GB, the Mn substitution has only a slight effect (<2%) on the overall atomic positions in the ferromagnetic (FM) Mn-Fe magnetic coupling case. For antiferromagnetic (AFM) Mn-Fe magnetic coupling, however, the Mn substitution induces an abrupt structural change in both the GB and FS, as shown in Tables I and II. The AFM Mn-Fe magnetic alignment is found to be the ground state in both the GB and FS environment. The metastable FM coupling is 0.30 and 0.80 eV/cell higher in energy than the AFM one for the GB and FS, respectively.

When we introduce the P impurity, remarkable effects are found from the comparison between the atomic structures of the Mn/Fe and (P+Mn)/Fe systems. In the GB case, the P-induced changes can be seen from the interlayer distance d_{23}, which increases by 0.74 a.u, and d_{34}, which shrinks by 0.45 a.u. In the FS case, a strong effect is also seen for d_{23} (increase by 0.62 a.u.) and d_{34} (decrease by 0.22 a.u.). As a result, the overall Mn-Fe(4) bond length increases by 0.20 and 0.34 a.u. for the GB and FS, respectively.

Comparing with P/Fe, the substitution of Mn in the GB has only a small interference effect on the atomic position of the surroundings (<2% in GB core). However, in the FS, the Mn adatom has a strong effect on the structure of the system. Compared to the atomic structure of the clean Fe(111) surface, the overall effect of Mn is to release the multilayer relaxation induced by P—the d_{12} increases (by 0.34 a.u.) and d_{23} shrinks (by 0.24 a.u.). Relative to the Fe(1)-Fe(4) bond length in the P/Fe FS (4.41 a.u.), the Mn-Fe(4) bond length is expanded by 0.24 a.u.

The structural relaxation is closely related to the change in electronic and magnetic properties. Indeed, it is found that the AFM Mn-Fe magnetic coupling, which serves as ground state in the binary Mn/Fe system, is no longer energetically favorable in the (P+Mn)/Fe GB and FS. For the FS, the total energy of the AFM Mn-Fe magnetic coupling is 0.40 eV/cell higher than in the FM Mn-Fe coupling configuration. For the GB, the Fe-Mn magnetic configuration in the GB center also changes from the initial AFM to a FM magnetic coupling.

More specifically, the calculated magnetic moment in each muffin-tin sphere listed in Tables III and IV shows that P and Mn strongly influence the magnetic properties in the Fe GB and FS. In the GB, the P impurity reduces the mag-

TABLE V. Calculated segregation energies (in eV) for Mn/Fe, P/Fe, and (P+Mn)/Fe systems. The chemical part is the result obtained without structural relaxation, the mechanical part is the interaction represented by the energy released during the relaxation of the clean Fe GB and FS after impurity removal, and the total interaction energy is the sum of these contributions.

System		ΔE_b	ΔE_s	$\Delta E_b-\Delta E_s$
Mn/Fe		−0.33 [a]	−0.53 [a]	+0.20
P/Fe	Unrelaxed (chemical)	−7.83	−7.74	−0.09
	Relaxation (mechanical)	+0.62	+0.36	+0.26
	Relaxed (total)	−7.21	−7.38	+0.17
(P+Mn)/Fe	Unrelaxed (chemical)	−8.21	−8.36	+0.15
	Relaxation (mechanical)	+1.07	+0.82	+0.25
	Relaxed (total)	−7.14	−7.54	+0.40

[a]For the substitutional case, ΔE_b and ΔE_s are computed as the change in system total energy upon replacement of an Fe atom with an Mn atom.

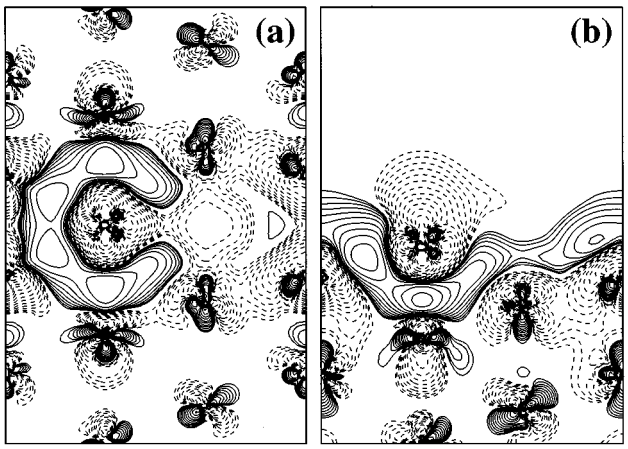

FIG. 2. The calculated valence charge density difference for (a) Mn/Fe GB and (b) Mn/Fe FS. Contours start from $\pm 5\times 10^{-4}$ e/a.u.^{3} and increase successively by a factor of $\sqrt{2}$. Solid contours denote charge accumulation and dashed lines denote charge depletion.

netic moment of Fe(3) by 0.37 μ_B (from 2.18μ_B to 1.81 μ_B). By contrast, P induces an enhancement of the magnetic moments of Fe(2) (by 0.20μ_B) and Fe(4) (by 0.12μ_B). At the FS, the local magnetic moment of Fe(3) is reduced by 0.19μ_B (from 2.10μ_B to 1.91μ_B). A small magnetic moment ($-0.04\mu_B$) is found on the P atom in both the GB and FS environments.

IV. SEGREGATION ENERGY AND CHEMICAL INTERACTION

The overall effects of Mn and P adatoms on the embrittlement of the FeΣ3(111) GB, according to the Rice-Wang model,[3] can be quantitatively determined through the magnitude and sign of the segregation energy difference $\Delta E_b - \Delta E_s$. The energy difference obtained for Mn substitution in the Fe GB and FS is +0.20 eV/adatom, indicating that Mn itself is a direct embrittler of the Fe GB. In addition, as listed in Table V, the calculated values (ΔE_b and ΔE_s) for P in P/Fe are -7.21 and -7.38 eV/adatom, giving an energy difference of +0.17 eV /adatom. Thus, by the Rice-Wang model, P and Mn serve as GB embrittlers of comparable potency. When the P impurities are added into the Fe GB and FS containing Mn, the ΔE_b and ΔE_s of P in the (P+Mn)/Fe GB and FS are found to be -7.14 and -7.54 eV/adatom. As a result, we obtain a positive segregation energy difference, $\Delta E_b - \Delta E_s = +0.40$ eV/adatom. From a comparison with the energy difference of P in P/Fe (+0.17 eV/adatom), the Mn alloying element significantly increases the embrittlement potency of P, in addition to the direct embrittlement by Mn.

It is instructive to compare the chemical and mechanical components in the binary P/Fe and ternary (P+Mn)/Fe systems. As listed in Table V, for both P/Fe and (P+Mn)/Fe, the atomic relaxation is very important for the energy difference $\Delta E_b - \Delta E_s$, as a negative value for the P/Fe system obtains if the structural relaxation for the clean GB is neglected. However, this mechanical component gives almost the same contribution for $\Delta E_b - \Delta E_s$ of the P impurity in P/Fe and in (P+Mn)/Fe. In contrast, the chemical contribution increases by 0.24 eV (from -0.09 to 0.15 eV) when we introduce the Mn alloying addition. Thus, it is the *chemical* energy which makes the primary contribution to the facilitating effect of Mn on P embrittlement.

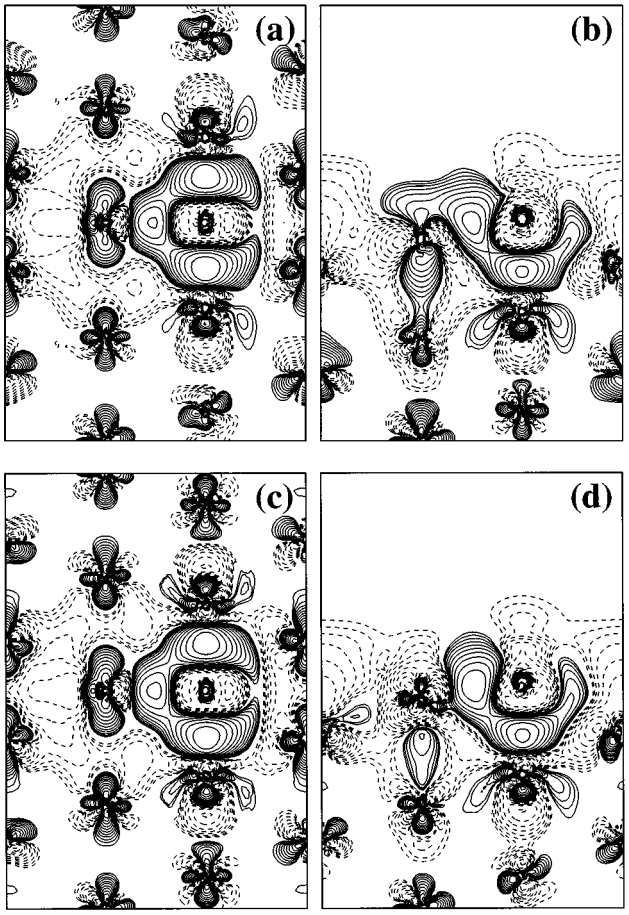

FIG. 3. The calculated valence charge density difference for (a) P/Fe GB, (b) P/Fe FS, (c) (Mn+P)/Fe GB, and (d) (Mn+P)/Fe FS. Contours start from $\pm 5\times 10^{-4}$ e/a.u.^{3} and increase successively by a factor of $\sqrt{2}$. Solid contours denote charge accumulation and dashed lines denote charge depletion.

To understand the chemical interactions underlying these energy differences, the charge-density differences plotted in the (110) plane are obtained by subtracting the superimposed charge densities of a free impurity monolayer and the reference systems (i.e., the GB or FS with the same geometry as in the systems considered but without impurity adatoms) from the self-consistent charge density for the corresponding systems. For binary Mn/Fe, as shown in Fig. 2, a pronounced charge accumulation between Mn-Fe(4) and Mn-Fe(2) is obvious for both the GB and FS environments, indicating a strong chemical interaction between the Mn and Fe neighbors. The contours around Fe(4) exhibit d_{z^2} character in both Figs. 2(a) and 2(b), which indicates the key role of this state in the Mn-Fe interaction. In the GB case, the interaction between the Mn and the Fe is limited to a short range due to screening effects. Since the bond length of Mn-Fe(2) (4.97 a.u.) is very close to that of Mn-Fe(4) (4.85 a.u.), the strength of the charge accumulation is very similar in the regions between Mn-Fe(2) and Mn-Fe(4). However, the Mn-Fe(4)

distance in the FS, 4.31 a.u., is much shorter than that in the GB. Thus, the charge accumulation between Mn and Fe(4) is much stronger than their counterpart in the GB, as shown in Fig. 2. [Quantitatively, in the region between Mn and Fe(4), the highest contour marks a charge of 0.016 electrons/$(a.u)^3$ in the FS, while in the GB it gives 0.008 electrons/$(a.u)^3$.] Relative to the GB case, the stronger charge accumulation in the FS is accompanied by an enhanced chemical interaction, thus causing the direct embrittlement by Mn.

The P-induced charge redistributions in the P/Fe GB and FS are plotted in Figs. 3(a) and 3(b); the corresponding figures for (P+Mn)/Fe are given in Figs. 3(c) and 3(d). Similarly, in all cases the charge density in the inner region around the P atom decreases. This apparent reverse charge transfer contradicts simple estimates made from electronegativity values (2.19 for P, 1.83 for Fe, and 1.55 for Mn) and indicates the nature of an embeddedlike interaction by which electrons redistribute within the P atoms. For the (P+Mn)/Fe GB and FS, the contour profile is similar to that for P/Fe except that the in-plane P-Mn bonding is stronger than that for P-Fe(1) in the P/Fe system. In the FS case, this is clear since the electrons are mainly located in-between P-Mn [c.f. Fig. 3(d)], while the interaction between P-Fe(1) shows a saturation behavior and the electrons begin to smear out into the vacuum region [cf. Fig. 3(b)]. In the GB case, the vertical interaction between P-Fe(3) is apparently weakened in (P +Mn)/Fe because of the enhanced in-plane P-Mn interaction. As a result, the bonding between P and the surrounding Mn and Fe atoms is more spatially isotropic in the (P +Mn)/Fe GB and FS.

From the previous study on metalloid impurities (B, C, P) in the Fe GB,[8] it was recognized that the spatial anisotropy of the impurity-Fe bonding is a crucial factor in determining the embrittlement potency. P is an embrittler in the P/Fe binary systems because the embedded-like P-Fe bonding is isotropic [the P-Fe(1) bonding is almost as strong as the P-Fe(3) bonding]. Going from GB to FS, only one of the Fe(3) near neighbors is removed. The bond energy lost due to the fracture should be significantly compensated through release of the lattice stress (relaxation energy) since only one out of five bonds is cut from the GB to FS. This argument can obviously be extended to the (P+Mn)/Fe systems as the further strengthened in-plane P-Mn bonding makes the P impurity interact more isotropically with the surrounding Mn and Fe atoms.

Generally, for metalloid impurities in the GB, the number of *p* electrons and the resulting spatial anisotropy of the bonding interaction between the impurity and the surrounding atom will tune the embrittlement behavior. Hence, it is very important to examine the complexities of chemical bonds in understanding the different effects of alloying elements. The simple argument that the effect of alloying elements on the P embrittling potency is determined by their relative electronegativities with respect to P and Fe does not appear to be relevant. On the other hand, the hybridization strength between metalloid impurity and transition metal additions may be an important parameter for the segregation and activity in the GB. Further investigations on the effect of Mn with B, C, and S on GB cohesion are in progress in order to verify the general validity of these arguments.

ACKNOWLEDGMENTS

Work supported by the Office of Naval Research (Grant No. N00014-94-1-0188) and a grant of computer time at the Pittsburgh Supercomputing Center from the NSF Division of Advanced Scientific Computing and the Arctic Region Supercomputing Center.

[1] G.B. Olson, in *Innovations in Ultrahigh-strength Steel Technology*, edited by G. B. Olson, M. Azrin, and E. S. Wright, Sagamore Army Materials Research Conf. Proc. No. 34 (U.S. GPO, Washington, D.C., 1990), p. 3.

[2] D. Y. Lee, E.V. Barrera, J. P. Stark, and H. L. Marcus, Metall. Trans. A **15A**, 1415 (1984).

[3] J.R. Rice and J-S. Wang, Mater. Sci. Eng. A **107**, 23 (1989); P.M. Anderson, J-S. Wang, and J.R. Rice, in *Innovations in Ultrahigh-strength Steel Technology* (Ref. 1), p. 619.

[4] C.L. Briant and R.P. Messmer, Philos. Mag. B **42**, 569 (1980), R.P. Messmer and C.L. Briant, Acta Metall. **30**, 457 (1982).

[5] M.E. Eberhart and D.D. Vvedensky, Scr. Metall. **22**, 183 (1988); J.M. MacLaren, S. Crampin, D.D. Vvedensky, and M.E. Eberhart, Phys. Rev. Lett. **63**, 2586 (1989).

[6] G.L. Krasko and G.B. Olson, Solid State Commun. **76**, 247 (1990).

[7] S. Tang, A. J. Freeman, and G.B. Olson, Phys. Rev. B **47**, 2441 (1993).

[8] R. Wu, A.J. Freeman, and G.B. Olson, Science **265**, 376 (1994); Phys. Rev. B **53**, 7504 (1996)

[9] In this notation, $\Sigma 3$ refers to a special orientation between crystals for which one in three lattice points is coincident, $[1\bar{1}0]$ denotes the crystal Miller indices of the axis of misorientation, and (111) denotes the habit plane of the boundary, both referred to the body-centered cubic crystal lattice of Fe. The boundary corresponds to the ''incoherent'' twin boundary.

[10] See, for example, J.M. Soler and A.R. Williams, Phys. Rev. B **40**, 1560 (1989); R. Yu, D. Singh, and H. Krakauer, Phys. Rev. B **43**, 6411 (1991).

[11] E. Wimmer, H. Krakauer, M. Weinert, and A.J. Freeman, Phys. Rev. B **24**, 864 (1981), and references therein.

[12] D.D. Koelling and B.N. Harmon, J. Phys. C **10**, 3107 (1977).

[13] U. von Barth and L. Hedin, J. Phys. C **5**, 1629 (1972).

[14] R. Wu and A.J. Freeman, Comput. Phys. Commun. **76**, 58 (1993).